

Impact of Thermal Reactor Radiation on Power Converter Circuit Performance

Matthew Niichel*, Stylianos Chatzidakis†

*2dLt, United States Space Force, Purdue University, 500 Central Dr, West Lafayette, IN 47907, mniichel@purdue.edu.

†PhD, Purdue University, 500 Central Dr, West Lafayette, IN 47907, schatzid@purdue.edu

INTRODUCTION

The increase in demand for renewable energy sources has driven several innovations in materials and electronics worldwide. Many of these sources, chiefly solar, operate off direct current (DC). One disadvantage of DC over alternating current (AC) is the inability to use transformers for voltage or current manipulations. While most small-scale electronics make use of DC voltages of 5 Volts or less, some applications require higher electric potential. This is especially true when integrating DC-generated renewables onto a grid designed for AC. Solid-state circuits, aptly named *boost converters*, are the DC analogous to step-up transformers where a higher potential is established at the expense of reduced current.

One application for boost converters is their use in creating a bias voltage for radiation detectors. A silicon photomultiplier (SiPM), when attached to a scintillating material, has replaced the need for large photomultiplier tubes, which has decreased the size of radiation detectors significantly. Similar to photomultiplier tubes, SiPMs require a high-voltage bias for operation. Often these detectors are powered by 5 Volt batteries, but the inclusion of a boost converter allows for a potential of nearly 100 Volts.

By nature, a radiation detector is subject to potentially damaging ionizing events. The boost converter circuit specifically, which makes use of a metal-oxide-semiconductor field effect transistor (MOSFET), is highly susceptible to radiation damage. This summary explores the ongoing efforts to explore the performance of the boost converter circuit under high gamma and neutron fluxes to design resilient radiation monitoring electronics. The live monitoring of a boost converter circuit placed within the Purdue University reactor (PUR-1) has given insight into the upper limits of radiation damage for boost converters.

BACKGROUND

The high voltage bias circuitry is a part of the Defense Threat Reduction Agency's Scatterable Radiation Monitor (SCRAM). [1] The SCRAM system has been a part of multiple system evaluations since 2023. [2] [3] The bias circuitry was identified as a critical system in the overall functionality of SCRAM, as it has the potential for radiation damage. The circuit makes use of the BS119n MOSFET. [2] Most boost converter circuits follow a similar component layout displayed in Fig 1. Not included in the schematic is the pulse width modulated driving circuit applied to the

MOSFET gate pin. Figure 2 displays the SCRAM chip with the accompanying Arduino power/measurement circuitry.

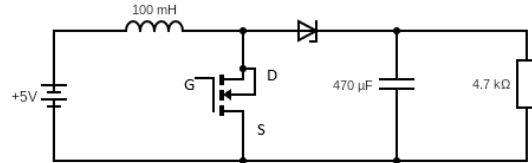


Fig 1. Generic boost converter circuit with N-channel enhancement type MOSFET.

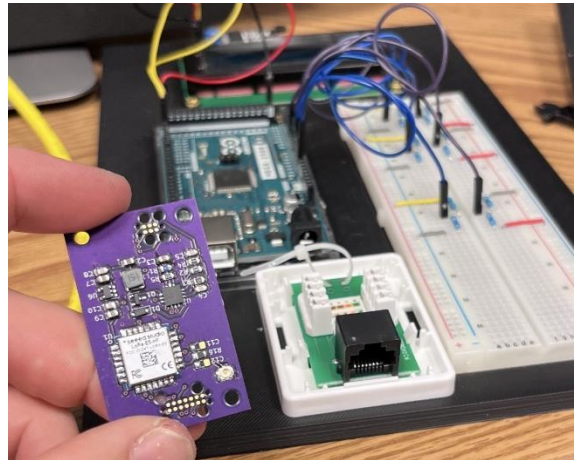


Fig 2. SCRAM chip with Arduino power supply and measurement circuitry.

It is widely accepted that gamma radiation affects MOSFETs by ionizing the oxide layers in the transistor. This minimizes the band gap, ultimately reducing the component's effectiveness as a switch by allowing current to leak. [4]

Less studied, but still of significance is damage induced by neutrons which typically cause a single-event burnout (SEB). The SEB is a large current state which ultimately causes a direct path from the source to drain without the need for gate bias.[5] However, the SEB is the worst case scenario for a MOSFET. It has been noted most frequently that the switching speed of the MOSFET is reduced as a function of induced neutron fluence. [6]

It is quite clear why complete failure of the MOSFET is problematic, however, of interest is the switching frequency reduction noted by multiple studies, and the subsequent affect that it renders on boost converters.

Neutron and gamma flux was administered to the SCRAM device from the PUR-1 reactor during live

monitoring. Additionally, a Co-60 irradiator was used in the evaluation of the circuit under pure gamma irradiation. However, physical limitations prevented the SCRAM from being powered on while under Co-60 irradiation. It is theorized that the addition of neutrons will induce a larger system level change in the SCRAM high voltage than by gammas alone due to the production of short-lived isotopes from activation. Future testing will include a means for shielding the SCRAM for neutrons while in the PUR-1 effectively establishing a pure gamma flux while powered on. This summary provides results from the irradiator and the combined neutron and gamma flux from PUR-1.

Boost Converter Operation

Boost converters operation can be divided into three steps centering around the switching of the MOSFET. 1) When the switch is open, current from the battery flows to the load through the inductor where it effectively acts as a wire. The capacitor is charged up to the voltage of the battery. 2) When the switch is closed, significantly more current travels through the inductor and returns *via* the short. The increase in current charges the inductor. 3) When the switch is reopened, the inductor applies a constructive potential to the capacitor allowing for a sum voltage charge of the inductor and the battery. The Zener diode then prevents the capacitor from discharging to the battery. The inductor potential follows equation (1). Where, V is inductor voltage, L is inductance, i is current, and t is the time.

$$V_L = L \frac{di}{dt} \quad (1)$$

The current component changes polarity for each state of the MOSFET switch. The time component for which the current changes is the time that the MOSFET remains in one state. The longer the switch is closed, the more time the inductor has to increase potential. Shown in equation (2), where R_b is the internal resistance of the battery.

$$V_L = V_0(1 - e^{-\frac{R_b t}{L}}) \quad (2)$$

When the switch is open, the inductor discharges. This follows equation (3).

$$V_L = V_0 e^{-\frac{R_L t}{L}} \quad (3)$$

For a MOSFET that has decreased switching frequency, there is a longer charge time and a shorter discharge time establishing an increased steady-state voltage. R_L is the load resistance.

METHODS

Co-60 Irradiator

The Purdue University Co-60 irradiator facility has a dose rate of 0.8 Gy/min (2024) calculated using *Fricke Dosimetry*. [7] Because the SCRAM system has several materials, it was assumed to be a generic plastic and the conservative energy of the gammas were assumed 1.5 MeV. Thus, the mass attenuation coefficient was determined to be

$2.76E-02 \text{ cm}^2/\text{g}$. Making use of equation (4), the dose rate of the SCRAM was found to be 0.96 Gy/min.

$$\dot{D}_{sample} = \dot{D}_{Fricke} \left[\frac{\mu_{en}^{sample}}{\mu_{en}^{water}} \right] \quad (4)$$

SCRAM was placed into the irradiator unpowered, and subsequently without live monitoring. An analysis was conducted post-irradiation in hopes of discovering damage of three SCRAM chips dwelling in the gamma flux for 10, 50, and 100 minutes. An inherent flaw with this set-up is that damage in MOSFETs is more probable during at power operation, due to applied currents. However, it is not impossible for damage to occur as oxide layers may be produced regardless of at power operations. The dwell times were selected by a set of design criteria set forth by DTRA, but there is utility in repeating the experiment for an increase in time by several orders of magnitude. The SCRAM chips, particularly the measured high voltage bias, was compared to control measurements conducted before irradiation. Additionally, an oscilloscope was used to measure the switching frequency across the drain and source of the MOSFET, once again comparing to the SCRAM chips prior to placement in the Co-60 irradiator.

Purdue-1 Reactor

The PUR-1 reactor is fitted with a 3-inch diameter drop tube which allows for the placement of the SCRAM device approximately 2 feet from the core. A container 3D printed out of ABS was constructed to place the chip and run the Cat5e cable for the purpose of powering the device and collecting signals. Figure 3 shows the drop tube with the Cat5e cable protruding.

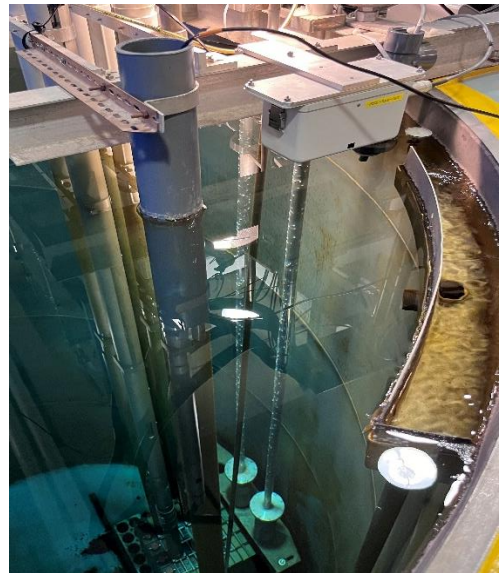


Fig.3. PVC drop tube leading down to PUR-1 in coolant well.

While the reactor is well characterized, the thermal and epithermal neutron flux was calculated by activating bare and cadmium covered gold foils at 1% reactor power. [8]

The actual flux was then determined by multiplying by 60 to match the 60% operational power during the experiments Table I provides the values of the experimental flux.

Table I. Measured Flux at 60% Reactor Power

Characteristic	Flux (n/cm ² *s)	Error
Total Average Flux	2.80E+07	1.57E+04
Average Thermal Flux	2.64E+07	3.45E+06
Average Epithermal Flux	1.73E+06	2.26E+05

The SCRAM chips placed in the reactor drop tube were evaluated until the Arduino collecting the data could no longer access the serial communication ports. This was considered the complete failure of the overall system. The average time for failure at 60% reactor power was 51 minutes with the maximum time at 68 minutes.

RESULTS

The Co-60 irradiator experiments proved to be uneventful in terms of any changes in the system performance when compared to the non-irradiated data. The nominal output for the high voltage is expected to be 34±1 Volt. The high voltage bias results are plotted in Figure 4 as a function of time where each sample number is 6 seconds.

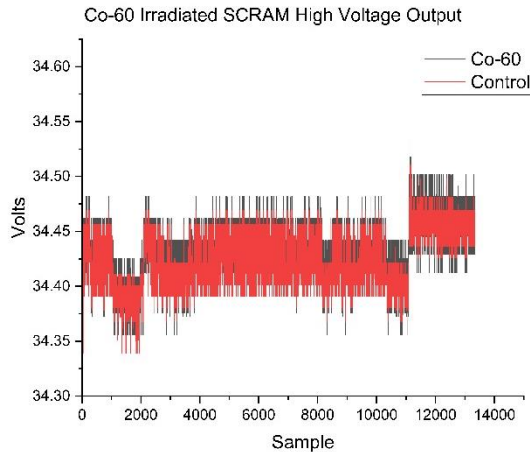


Fig. 4. Measured SCRAM high voltage bias following Co-60 irradiation.

The SCRAM chips placed in PUR-1 displayed a significantly more interesting behavior during irradiation when compared to the control and Co-60 experiment. These results are plotted as a function of neutron fluence to express where the potential damage occurred. Two additional SCRAM chips were placed under the same conditions in the reactor, but lost communication earlier than the chip displayed in Figure 5. The total amount of time in the drop tube at 60% power was 68 minutes prior to communication failure. It is important to note, that the SCRAM displayed in Figure 5 was operated one week from the removal of the reactor and the high voltage output was measured to be 41.2 Volts on average. The output voltage remained high relative to the control chips.

SCRAM High Voltage Bias Under 60% Power of PUR-1

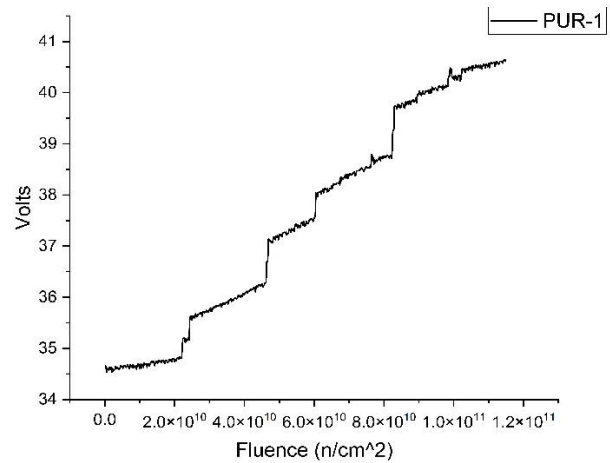


Fig. 5. SCRAM high voltage while in PUR-1 drop tube as a function of neutron fluence.

In an effort to evaluate the theory that the MOSFET was the source of increased output voltage. An oscilloscope was used to measure the switching frequency by placing the terminals across the drain and source leads of the MOSFET while power was applied to SCRAM. A control measurement was taken shown in Figure 6. The measurement of the SCRAM placed in PUR-1 is shown in Figure 7. The SCRAM chips placed in the Co-60 irradiators were measured in the same fashion, however, the average of the switching frequency was 298± 5 kHz. This was not a significant enough change from the control measurements to warrant mentioning.

Considering the results presented in Figure 6 and 7, when the signal is pegged high, this is indicative of the switch being closed, as the full voltage is dropped across the terminals. The switch is closed when the voltage is measured at the low steady-state. There is still some voltage dropped across the MOSFET due to internal resistance.

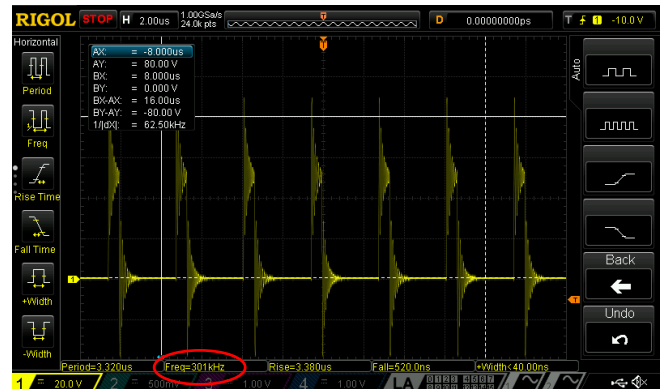


Fig. 6. Measured drain-source switching frequency of MOSFET for control SCRAM.

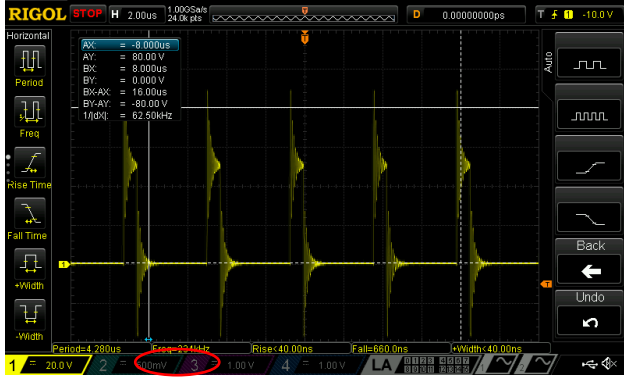


Fig. 7. Measured drain-source switching frequency of MOSFET for PUR-1 tested SCRAM.

As shown in the oscilloscope measurements, the switching frequency of the SCRAM placed in PUR-1 is reduced by nearly 70 kHz. A waveform analysis allows for the approximate determination of the MOSFET on and off times. These values are presented in Table II.

Table II. MOSFET Switching time for SCRAM chips

SCRAM	On-Time (μS)	Off-Time (μS)
Control	2.8	0.56
PUR-1	3.6	0.72

Given that the inductor is the critical component in the boost converter circuit which affects the output voltage, we can consider the ratio of the charging from equation (2) and the off-time presented in Table II, to calculate the predicted output ratio for a damaged SCRAM from PUR-1. Equation (5) displays the ratio. Equation (6) multiples the ratio calculated to find the predicted measured output.

$$\frac{e^{-0.56}}{e^{-0.72}} = 1.174 \quad (5)$$

$$1.174 * 35 \text{ Volts} = 41.1 \text{ Volts} \quad (6)$$

CONCLUSION

Boost converter circuits are an integral aspect of modern society. At their heart, is the MOSFET type transistor which has long been known for its sensitivity to radiation damage. While there is more information available for gamma induced damage than neutrons, both have been identified to cause issues. This series of experiments aims to explore how both gammas and neutrons affect the boost converter output by way of damage to the MOSFET.

In this summary, several SCRAM chips which make use of a boost converter were evaluated under Co-60 gamma flux and placed in the Purdue University reactor. Due to physical constraints, the SCRAM devices could not be powered while in the Co-60 irradiator. As a result, it is theorized that the results from the Co-60 are not fully realized. However, the results measured from PUR-1 provide strong evidence for damage to the MOSFET which in turn, drastically increases boost converter output voltages.

Much work is still needed to determine which type of radiation inflicts more damage to the SCRAM's functionality. A promising prospect includes making use of the PUR-1 reactor while shielding neutrons through cadmium. Continued efforts will hopefully provide such insight, not only for the SCRAM project, but any device which utilizes a boost converter circuit.

ACKNOWLEDGMENTS

This research was performed using the Purdue College of Engineering and Purdue Military Research Institute funding. A special thank you to Major Fobar, USA of Nuclear Science & Engineering Research Center at West Point, NY.

DISCLAIMER

The views expressed in this article are those of the author and do not reflect the official policy or position of the United States Air Force, Department of Defense, or the U.S. Government.

REFERENCES

- [1] D. Fobar, *Scatterable Radiation Monitor (SCRAM) Purdue Version*.
- [2] M. Niichel, "Development of An Electronics Testbed for Radiation Testing In Gamma And Neutron Environments," Purdue University, West Lafayette, IN, 2024.
- [3] M. Niichel and S. Chatzidakis, "Methodology for the Evaluation of Critical Components of the Scatterable Radiation Monitor Under Radiation Fields," *TRANSACTIONS*, Nov. 2024, doi: doi.org/10.13182/T131-45979.
- [4] C. L. Wilson and J. L. Blue, "Two-Dimensional Modeling of N-Channel MOSFETs including Radiation-Induced Interface and Oxide Charge," *IEEE Trans. Nucl. Sci.*, vol. 31, no. 6, pp. 1448–1452, Dec. 1984, doi: 10.1109/TNS.1984.4333528.
- [5] Q. Zeng, Z. Yang, X. Wang, S. Li, and F. Gao, "Research Progress on Radiation Damage Mechanism of SiC MOSFETs Under Various Irradiation Conditions," *IEEE Trans. Electron Devices*, vol. 71, no. 3, pp. 1718–1727, Mar. 2024, doi: 10.1109/TED.2024.3359172.
- [6] L. Mo *et al.*, "Single event burnout of SiC MOSFET induced by atmospheric neutrons," *Microelectronics Reliability*, vol. 146, p. 114997, Jul. 2023, doi: 10.1016/j.microrel.2023.114997.
- [7] "Purdue University Co-60 Irradiator." Radiological and Environmental Management, Dec. 12, 2024.
- [8] Matthew Niichel *et al.*, "Design and Characterization of the Modified Purdue Subcritical Pile for Nuclear Research Applications," *Pre-Print*.